

## Visual Curvature

HaiRong Liu<sup>1</sup>, Longin Jan Latecki<sup>2</sup>, WenYu Liu<sup>1</sup>, Xiang Bai<sup>1</sup>  
 HuaZhong University of Science and Technology, P.R. China<sup>1</sup>

Temple University, USA<sup>2</sup>

lhrbss@gmail.com, latecki@temple.edu, liuwy@hust.edu.cn, xiang.bai@gmail.com

### Abstract

In this paper, we propose a new definition of curvature, called visual curvature. It is based on statistics of the extreme points of the height functions computed over all directions. By gradually ignoring relatively small heights, a single parameter multi-scale curvature is obtained. It does not modify the original contour and the scale parameter has an obvious geometric meaning. The theoretical properties and the experiments presented demonstrate that multi-scale visual curvature is stable, even in the presence of significant noise. In particular, it can deal with contours with significant gaps. We also show a relation between multi-scale visual curvature and convexity of simple closed curves. To our best knowledge, the proposed definition of visual curvature is the first ever that applies to regular curves as defined in differential geometry as well as to turn angles of polygonal curves. Moreover, it yields stable curvature estimates of curves in digital images even under sever distortions.

### 1. Introduction

Curvatures of curves are the key to detect the salient points and to compute the shape descriptors. Mathematically, curvature of a point  $v$  is defined as following:

$$K(v) = \lim_{\Delta S \rightarrow 0} \left| \frac{\Delta \theta(v)}{\Delta S} \right| \quad (1)$$

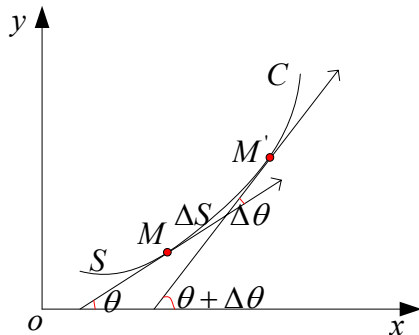


Figure 1. Curvature of the curve

where  $\theta(v)$  is the tangential angle of the point  $v$  and  $S$  is the arc length.

When applied in digital images, three problems arise:

- (1) The digital images are usually distorted by noise. Fig. 2(a) can be regarded as a pentagram heavily distorted by noise; Fig. 2(b) is the pentagram without noise. For the visual perception, point  $A$  is not important, because it should be flat there. However, the curvature computed by formula (1) can be very high.

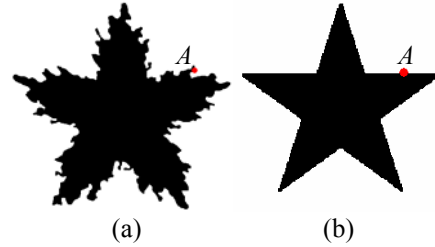


Figure 2. Pentagram

- (2) The images may have different level of details. If Fig. 2(a) is regarded as an image that looks like a pentagram in global, the curvature of point  $A$  should be low in the large scale; at the same time, because there is a very sharp turn in small scale, the curvature should be high. Obviously, formula (1) is hard to compute the curvature in different scales.
- (3) Due to digitalization, the contours of the images are all stair-like, such as Fig. 3. In such case, formula (1) cannot be directly applied.



Figure 3. Stair-like contour

From the point of visual perception, the curvature estimated in certain level must get rid of the influence of the convex and concave parts in smaller levels.

The contour can be parameterized by arc length:

$$C(s) = (x(s), y(s)) \quad (2)$$

We call  $x(s)$  the height function in  $0^\circ$  direction and  $y(s)$  the height function in  $90^\circ$  direction. The intuition is that  $x(s)$  measures the distance to  $y$ -axis in  $0^\circ$  direction. Rotate the coordinate system by angle  $\alpha$  anticlockwise, the new  $x(s)$  becomes the height function of the contour in direction  $\alpha$ , which we denote  $H_\alpha$ . Since the height function is defined as distances to rotated  $y$ -axis, and the direction of  $y$ -axis does not matter, we restrict  $\alpha \in [0, \pi)$ . By rotating the coordinate system by angle  $\alpha_i = \pi \frac{i}{N}, i = 0, \dots, N-1$ , we obtain a series of height functions  $H_{\alpha_i}$ .

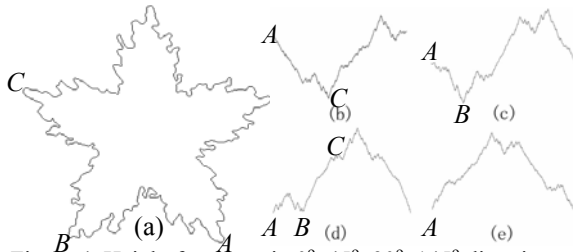


Figure 4. Height functions in  $0^\circ, 45^\circ, 90^\circ, 145^\circ$  directions

Fig. 4(b), (c), (d), (e) shows the height functions of the contour in (a) in  $0^\circ, 45^\circ, 90^\circ, 145^\circ$  directions, respectively. Every height function reflects partial information of the contour. The curvature is related to the local extreme points of the height functions: In more directions the point is the extreme points, the sharper the contour is at the point, i.e. point  $A$ , the higher is the curvature of the point. The main idea of this paper is to define the curvature at a contour point  $v$  by counting the number of directions in which  $v$  is an extremum of the height function.

Obviously, all of the extreme points are not of the same importance. Noise may perturb the curve and cause small extreme points in the height functions. However, a point on a small concave or convex part can not become an obvious height in any height functions, while a point on a large concave or convex part will be an obvious height in some height functions. For example, in Fig. 4(d),  $A$  and  $B$  are the very important extreme points and  $C$  is not so important, but  $C$  is a very important minimum point in Fig. 4(b). When the number of height functions is sufficiently large, no important points are ignored, and important high curvature points are detected. In this paper, we obtain multi-scale curvature by ignoring small heights in the height functions.

The new definition for curvature, called visual curvature, is based on statistics of the extreme points of the height functions computed over all directions. Moreover, by gradually ignoring relatively small heights, multi-scale curvature is constructed. The multi-scale visual curvature has the following properties:

- (1) It is suitable for every planar curve. When the number of the height functions approaches infinite, on the regular curve, its limit is standard curvature and on the polygonal curve, it is identical to turn angle.

- (2) It forms a single parameter scale space. Curvature is obtained by ignoring small heights, not by smoothing. Hence it does not modify the original curve.

The related literatures are reviewed in Section 2. In Section 3, the visual curvature is defined and its relation to standard curvature and turn angle has been proved. In Section 4, a scale measure of extreme point is defined in the point of absolute extreme. In Section 5, some properties of multi-scale visual curvature are described and their significances are discussed. In Section 6, implementation details are analyzed and the experimental results are demonstrated. In Section 7, we describe some applications of the visual curvature. In Section 8, we draw a conclusion of this paper.

## 2. Literature Review

Curvature estimation in digital images is known to be very susceptible to noise on the contour, thus it is very hard to estimate it robustly. Since large number of methods has already been proposed for estimating the curvature of contour, it is beyond the scope of this paper to list all of them. Therefore, we mention only a few beginning with a very influential method from the early days of computer vision [10] through methods in [1, 2, 3, 4, 5, 6]. Those approaches can be classified into three groups, according to definition of curvature they are using: tangent direction, osculating circle, derivation. Most methods use a sliding window, thus they in essence estimate the curvature locally. The size of the sliding window is usually hard to choose and when noise is large, simply increasing the size of sliding window usually does not work. At the same time, these methods are all under the assumption that there is a unique curvature at each point which is obviously true in pure mathematical view. However, in the context of computer vision, depending on particular goals, the curvature of a point may take on differing values, e.g., depending on whether a given point is regarded as noise or signal point.

Before describing the existing multi-scale curvature techniques, we characterize the desirable properties of the curvature that is useful in computer vision: (1) it should be multi-scale and reflect the curvature information of the contour in different scale; the geometric meaning of the scale factor should be as clearly as possible which facilitates the selection of scale in the application; (2) it should have proper precision; (3) it should be stable under noise; (4) it should be invariant under rotations and translations. (5) it should be suitable for both smooth curves and polygonal arcs.

The main goal of this paper is to propose a new curvature definition which will achieve all the above properties. To our best knowledge, no existing multi-scale curvature has all these properties. Our proposed multi-scale curvature is easy to implement, and can be computed efficiently.

The following is a brief review of existing multi-scale curvature techniques. In computer vision, multi-scale curvature is usually related to multi-scale shape representation techniques.

Mokhtarian and Mackworth [7] proposed a multi-scale, curvature based shape representation technique by convolving the contour with a Gaussian kernel. They demonstrated many of its appealing properties. However, this method modifies the original curve. At the same time, the geometric meaning of its scale factor which is in fact a parameter of Gaussian kernel is not obvious. A similar method [8], which is proposed by Yu-Ping Wang, convolves the contour with a dilated-spline kernel. Since just kernel function is altered, they share the same problems.

Latecki and Rosenfeld [9] proposed a class of planar arcs and curves which is general enough to describe (parts of) the boundaries of planar real objects. They analyzed the properties of these arcs and ruled out pathological arcs, thus simplify the shape representation problem. A popular way of shape representation in digital grid is curvature based polygonal approximation [11, 12, 13, 14, 15]. In these methods, the original contour is approximated by simplified polygon. Obviously, in polygonal arcs, a natural measure of curvature information is turn angle. The problem with standard curvature is that it is defined on smooth curve and can not be applied to polygonal arcs directly. Thus, they need complicated estimation procedure to calculate curvature.

To summarize, although there are many methods to obtain multi-scale curvature, they in essence estimate the curvature from the definition of standard curvature or its properties. Thus, they usually need to smooth the polygonal arcs, either by curve fitting or by convolution. This results in parameters that are hard to control, such as the size of sliding window, and displacement of contour points which is usually not desirable.

### 3. Visual Curvature

As described in Section 1, by rotating the coordinate system, we can obtain a series of height functions

$$H_{\alpha_i}, \alpha_i = \pi \frac{i}{N}, i = 0, \dots, N-1.$$

**Definition 1.** For a point  $v$  on the curve  $C$ , suppose  $S(v)$  is its neighborhood of size  $\Delta S$  on the curve  $C$ , the visual curvature of  $v$  is defined as:

$$K_{N,\Delta S}(v) = \pi \frac{\sum_{i=0}^{N-1} \# [H_{\alpha_i}(S(v))]}{N\Delta S} \quad (3)$$

where  $\# [H_{\alpha_i}(S(v))]$  represents the number of local extreme points of the height function  $H_{\alpha_i}$  in the neighborhood  $S(v)$ .

This definition also points out how to compute the visual

curvature. For a point  $v$  on the contour, we estimate its curvature in its small neighborhood  $S(v)$ . In every height function, we find its extreme points and count the number of the extreme points that are in the neighborhood  $S(v)$ . We sum up all the numbers and calculate the curvature using formula (3). As we will report later in the section on experimental results, keeping  $\Delta S=1$ , i.e.,  $S(v)=\{v\}$ , yields the most robust curvature estimate for digital contours in real images. We did not restrict the size  $\Delta S$  of the neighborhood of point  $v$  in formula (3) for theoretical reasons, in particular, to formulate Theorem 1 below in its general form. This theorem reveals the relation between visual curvature and the standard curvature on the regular curve. It states that when the number of the height functions is sufficiently large, the visual curvature approaches the standard curvature. Regular curve is a curve which is differentiable and the derivative never vanishes.

**Theorem 1.** For a point  $v$  on the regular curve  $C$ , we have

$$K(v) = \lim_{\Delta S \rightarrow 0} \lim_{N \rightarrow \infty} K_{N,\Delta S}(v) \quad (4)$$

**Proof:** Let  $\theta$  be the tangent angle at point  $v$ . Assume  $\theta \neq 0$ . If  $\theta=0$ , we rotate the coordinate system so that it satisfies this assumption. Since the curve is regular, by properly rotating coordinate system, there exists a neighborhood  $S(v)$  such that the range of the tangent angle in this neighborhood is a subset of the half-open interval  $[0, \pi)$ , devoted by  $(\theta_1, \theta_2)$ . See Fig. 5 below.

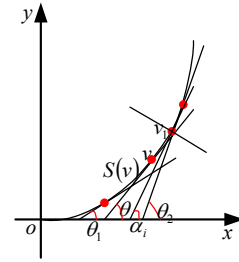


Figure 5. Relation between tangential angle and extreme point

If a point  $v_1 \in S(v)$  is the extreme point of the height function  $H_{\alpha_i}$ , then  $\alpha_i \in (\theta_1, \theta_2)$  and vice versa. Hence the number of the extreme points of all the height functions in the neighborhood  $S(v)$  is identical to the number of direction angles  $\alpha_i$  that belong to the open interval  $(\theta_1, \theta_2)$ .

The direction angle series  $\left\{ \alpha_i = \frac{\pi i}{N} \mid i = 0, \dots, N-1 \right\}$  of the height functions is a uniform sampling of the half-open interval  $[0, \pi)$ . Suppose  $\alpha_n = \pi n/N$  and  $\alpha_m = \pi m/N$  are the smallest and largest sampling direction angles in the open interval  $(\theta_1, \theta_2)$ , respectively. Then  $\pi(m-n+1)/N$  is an estimation of  $\theta_2 - \theta_1$ .

We now prove that the limit of  $\pi(m-n+1)/N$  is  $\theta_2 - \theta_1$  when  $N$  approaches infinity. We just need to show that

$$(a) \pi \lim_{N \rightarrow \infty} \frac{m}{N} = \theta_2 \quad (b) \pi \lim_{N \rightarrow \infty} \frac{n}{N} = \theta_1$$

Both (a) and (b) can be proved in the same way, thus, we just prove (a). Because  $\alpha_m = \pi m/N$  is the largest angle in the set  $\left\{ \alpha_i = \frac{\pi i}{N} \mid i = 0, \dots, N-1 \right\}$  which is in interval  $(\theta_1, \theta_2)$ , then  $\alpha_m = \pi m/N \leq \theta_2$  and  $\alpha_{m+1} = \pi(m+1)/N > \theta_2$ ,

$$\lim_{N \rightarrow \infty} |\alpha_m - \theta_2| \leq \lim_{N \rightarrow \infty} |\alpha_m - \alpha_{m+1}| = \pi \lim_{N \rightarrow \infty} \frac{1}{N} = 0$$

$$\pi \lim_{N \rightarrow \infty} \frac{m}{N} = \lim_{N \rightarrow \infty} \alpha_m = \theta_2$$

Therefore,

$$\lim_{\Delta S \rightarrow 0} \lim_{N \rightarrow \infty} K_{N, \Delta S}(v) = \lim_{\Delta S \rightarrow 0} \lim_{N \rightarrow \infty} \pi \frac{\sum_{i=0}^{N-1} \# [H_{\alpha_i}(S(v))]}{N \Delta S} = \lim_{\Delta S \rightarrow 0} \frac{\theta_2 - \theta_1}{\Delta S} = K(v)$$

The theorem below reveals the relation between visual curvature and turn angle of polygonal curves. We first motivate this theorem with an example. In Fig. 6,  $MON$  is part of the polygonal curve, the turn angle at  $O$  is  $\alpha$ .  $t$  is a line whose directional angle, denoted by  $\beta_t$ , is in the interval  $(0, \alpha)$  and  $l$  is a line whose directional angle, denoted by  $\beta_l$ , is in the interval  $(\alpha, \pi)$ . Obviously,  $O$  is an extreme point of height function in the direction  $\pi/2 + \beta_t$  which is perpendicular to  $t$ , but it is not an extreme point of height function in the direction  $\pi/2 + \beta_l$  which is perpendicular to  $l$ . Thus, in Fig. 6, in the direction perpendicular to  $\beta \in (0, \alpha)$ ,  $O$  is an extreme point and total range of  $\beta$  is  $\alpha$ .

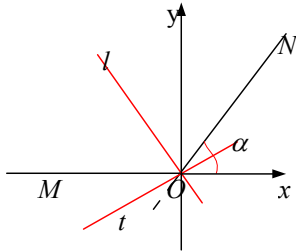


Figure 6. Relation between visual curvature and turn angle

**Theorem 2.** For a point  $O$  with turn angle  $\alpha(O)$  on a polygonal curve, we have

$$\alpha(O) = \lim_{N \rightarrow \infty} K_{N,1}(O) \quad (5)$$

**Proof:** Since  $\Delta S=1$ , we just need to count the number of height functions in which  $O$  is an extreme point. Let us assume that there are  $N$  height functions and  $O$  is an extreme point of  $M$  height functions. Then  $\pi M/N$  is an estimation of the range of the angle in which direction  $O$  is an extreme point. As illustrated in Fig. 6, such range is  $\alpha$ . Following the proof of theorem 1, we can show:

$$\alpha(O) = \pi \lim_{N \rightarrow \infty} \frac{M}{N} = \lim_{N \rightarrow \infty} K_{N,1}(O)$$

#### 4. A Scale Measure of Extreme Point

In Def. 1, all extreme points are counted, not considering whether they are important or not. Therefore, Theorem 1 also explains why standard curvature is not robust. In fact, in a certain scale, small concave or convex parts should be ignored. By imposing a scale measure for extreme point, the multi-scale visual curvature can be defined as follows:

**Definition 2.** For a point  $v$  on a curve  $C$ , suppose  $S(v)$  is its neighborhood of size  $\Delta S$  on the curve  $C$ , the multi-scale visual curvature of the point  $v$  is defined to be:

$$K_{N, \Delta S}^\lambda(v) = \pi \frac{\sum_{i=0}^{N-1} \# [H_{\alpha_i}^\lambda(S(v))]}{N \Delta S} \quad (6)$$

Where  $\lambda$  is a scale factor and  $\# [H_{\alpha_i}^\lambda(S(v))]$  represents the number of the extreme points of the height function  $H_{\alpha_i}$  in the neighborhood  $S(v)$  whose scale measure is not smaller than  $\lambda$ . In short, the multi-scale visual curvature is computed by counting the number of relative important extreme points. The scale measure  $\lambda$  can be defined in different ways. Definition 5 below presents our choice. The intuition is that in every height function, the higher the peak represented by the extreme point is, the more important the extreme point is. We begin with a definition of a measure that quantifies the heights of peaks.

**Definition 3.** The influence region of a local maximum (minimum) point  $v$  in a height function  $H_\alpha$ , denoted by  $R_\alpha(v)$ , is its maximal neighborhood such that the height of every point in this neighborhood is not higher (lower) than the height of the point  $v$ . If curve  $C$  is open or point  $v$  is not an absolute extremum,  $R_\alpha(v)$  is divided into two segments by  $v$ , we denote the left segment by  $R_\alpha^-(v)$  and the right segment by  $R_\alpha^+(v)$ , see Fig. 7. If curve  $C$  is closed,  $R_\alpha(v)$  may be the whole curve, in which case  $R_\alpha^-(v)$  and  $R_\alpha^+(v)$  both represent the whole curve except point  $v$ , in particular,  $R_\alpha(v) = R_\alpha^+(v) = R_\alpha^-(v)$ .

**Definition 4.** The height of the peak represented by an extreme point  $v$  in the height function  $H_\alpha$ , denoted by  $r_\alpha(v)$ , is defined as:

$$r_\alpha(v) = \min[r_\alpha^+(v), r_\alpha^-(v)] \quad (7)$$

$$r_\alpha^+(v) = \max \{ H_\alpha(p) - H_\alpha(v) \mid p \in R_\alpha^+(v) \}$$

$$r_\alpha^-(v) = \max \{ H_\alpha(p) - H_\alpha(v) \mid p \in R_\alpha^-(v) \}$$

$r_\alpha^+(v)$  and  $r_\alpha^-(v)$  are the maximal height differences between  $v$  and the points belonging to  $R_\alpha^+(v)$  and  $R_\alpha^-(v)$ , respectively.

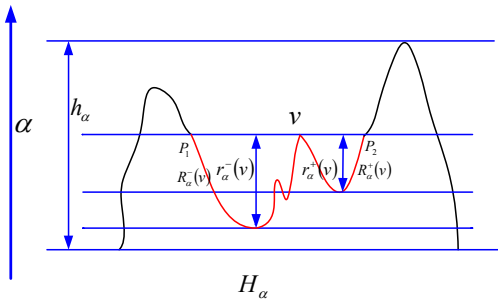


Figure 7. Influence region and the height of peak

In Fig. 7,  $v$  is a local maximum point, the curve segment  $P_1P_2$  which is in red is its influence region, the curve segment  $vP_1$  is the left segment of the influence region and curve segment  $vP_2$  is the right segment of the influence region. Obviously, whether a peak is important or not, depends not only on the height of this peak, but also on the scale of the contour or the image. In the definition below, it is compared to the height of  $H_\alpha$ , denoted by  $h_\alpha$ , which is the height difference between the absolute maximum point and the absolute minimum point of  $H_\alpha$ . However, we could define it in different ways according to applications.

**Definition 5.** The scale measure of an extreme point  $v$  in the height function  $H_\alpha$ , denoted by  $\lambda_\alpha(v)$ , is the height of the peak represented by  $v$  divided over the height of  $H_\alpha$ :

$$\lambda_\alpha(v) = \frac{r_\alpha(v)}{h_\alpha} \quad (8)$$

The scale measure of a point  $v$  represents in which scale in direction  $\alpha$ ,  $v$  can be considered to be important. According to the definition,  $\lambda_\alpha(v) > 0$ .

**Definition 6.** The representative scale measure of a point  $v$ , denoted by  $\lambda(v)$ , is the maximum of its scale measures in all the height functions.

For a contour point, in the scale larger than its representative scale measure, its visual curvature vanishes and the convex or concave part represented by this point is ignored.

## 5. Properties of Multi-scale Visual Curvature

This section presents a number of important results on the multi-scale visual curvature. It also discusses the practical significance of each of those results. The properties below are all under the assumption that the number of the height functions is sufficiently large, thus none of important extreme point is ignored.

**Theorem 3.** As the scale factor  $\lambda$  increases, the multi-scale visual curvature of a point is non-increasing.

Theorem 3 is a natural result of the definition of multi-scale visual curvature. It shows that an unimportant contour point in a certain scale is also unimportant in a higher scale.

**Theorem 4.** Multi-scale visual curvature is invariant under rotation and translation. If the size  $\Delta S$  in formula (6) is proportional to the whole length of the contour, it is also invariant under uniform scaling.

This invariance property is very essential since it make it possible to compute the shape descriptors from multi-scale visual curvature.

**Theorem 5.** Let  $C$  be a closed planar curve and let  $G$  be the boundary curve of its convex hull,  $v$  is a point on the curve  $C$ . Then

- (1)  $v \in G$  if and only if  $\lambda(v) = 1$
- (2)  $v \notin G$  if and only if  $\lambda(v) < 1$

In the digital images, the contour  $C$  is in fact a polygon with finite vertices  $\{V_i | i=1, \dots, N\}$ , where  $N$  is the number of the vertices. Let  $G$  be the boundary curve of the convex hull of  $C$ . For a contour segment defined by vertices  $\{V_i | i=m, \dots, n\}$  with  $V_m$  and  $V_n$  being its two end points, we call it a concave segment if all the points except the two end points on the segment do not belong to  $G$ .

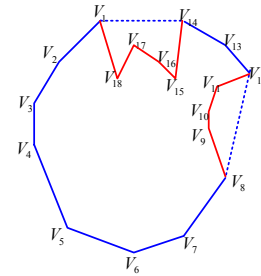


Figure 8. The concave segments

In Fig. 8, there are two concave segments,  $V_1V_{18}V_{17}V_{16}V_{15}V_{14}$  and  $V_8V_9V_{10}V_{11}V_{12}$ . Obviously, by substituting all concave segments with the line segments connecting their two end points, we obtain the convex hull of the polygon.

**Definition 7.** The scale measure of a concave segment  $\Gamma$ , denoted by  $\lambda(\Gamma)$ , is the maximum of the representative scale measure of the points which belong to  $\Gamma$  except the two end points.

In Fig. 8, the scale measures of the two concave segments are:

$$\lambda(V_8V_9V_{10}V_{11}V_{12}) = \max\{\lambda(V_9), \lambda(V_{10}), \lambda(V_{11})\}$$

$$\lambda(V_1V_{18}V_{17}V_{16}V_{15}V_{14}) = \max\{\lambda(V_{18}), \lambda(V_{17}), \lambda(V_{16}), \lambda(V_{15})\}$$

Since except the two end points, the points which belong to  $\Gamma$  do not belong to the convex hull, according to Theorem 5,  $\lambda(\Gamma) < 1$ .

**Definition 8.** Given a scale threshold  $\lambda$ , for a closed polygon  $C$ , deletes all the vertices  $V$  where the visual curvature vanishes and connects the remaining vertices in sequence. The new polygon is called a  $\lambda$ -scale approximation of  $C$ , denoted by  $C_\lambda$ .

**Theorem 6.** On the  $C_\lambda$ , all the concave segments which scale measures are smaller than  $\lambda$  are substituted by the line

segments connecting their two end points. Specially,  $C_0=C$  and  $C_1=G$ .

Theorem 6 is a natural result of Def. 7 and Def. 8. It shows that as  $\lambda$  increases, more concave segments are ignored and  $C_\lambda$  becomes simpler until it converges to the boundary curve of its convex hull. It also points out how to select the scale threshold  $\lambda$  in the applications: the scale threshold depends on the scale of the concave segments we want to ignore.

## 6. Implementation Details and Experimental Results

Because of digitalization, some high curvature points may disappear. Let us consider two example cases in Fig. 9.

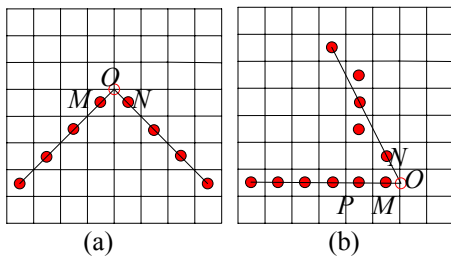


Figure 9. High curvature point disappears

In Fig. 9(b), the turn angle at point  $O$  is about  $117^\circ$ ; however, point  $O$  is not represented by a pixel at the same location. The digitalization process mapped it to one of digital points  $M$  and  $N$  or possibly to both of them. Neither the visual curvature at  $M$  nor at  $N$  is equal to the curvature of  $O$ , but their sum is. This observation motivates the following approach to compute visual curvature in digital images.

For a given scale  $\lambda$  and a given threshold  $T$ , for every point  $v$  we consider its neighborhood  $U(v)$  of radius  $T$ . If the representative scale measure  $\lambda(v)$  is the largest among all points in  $U(v)$ , then the new digital visual curvature at  $v$  is sum of all curvature values in  $U(v)$ , i.e.,

$$DK_{N,\Delta S}^\lambda(v) = \sum_{u \in U(v)} K_{N,\Delta S}^\lambda(u) \quad (9)$$

At the same time we set the digital visual curvature value of all other points in  $U(v)$  to zero. Actually, we compute in formula (9) the total curvature over the arc determined by the neighborhood  $U(v)$ , and assign it to a single point.

Now we illustrate on our example in Fig. 9 that there exists a digital point whose visual curvature best represents the original point  $O$ . After digitalization,  $O$  disappears and its information is lost. However, the turn angle of  $M$  and  $N$  is high in a relative high scale, such as  $\lambda=0.01$ . Point  $M$  is selected as best representing  $O$  based on the fact that  $\lambda(M) > \lambda(N)$  and the distance between  $M$  and  $N$  is less than  $T$ . We show that the proposed approach modifies the curvature of  $M$  to be the curvature of  $O$  in the original continuous contour. For simplicity, let us assume that

neighborhood  $U(M)$  just contain  $P, M, N$ . We obtain

$$DK_{N,\Delta S}^\lambda(M) = K_{N,\Delta S}^\lambda(M) + K_{N,\Delta S}^\lambda(N) + K_{N,\Delta S}^\lambda(P)$$

$$\text{and } DK_{N,\Delta S}^\lambda(N) = DK_{N,\Delta S}^\lambda(P) = 0$$

The computed digital visual curvature of  $M$  is  $117/180\pi$ . According to Theorem 2, this yields correctly the value of about  $117^\circ$  for the turn angle of  $M$ . The justification for this is as follows. In a height function  $H_\alpha$ , if one of the points among  $P, M$  and  $N$  is an extreme point, we increase the count number of  $M$ . From the figure, we can observe that if  $O$  is an extreme point of the height function of the original continuous object in direction  $\alpha$ , then either  $M$  or  $N$  will be an extreme point of the height function of the digital object in direction  $\alpha$ . Thus, the computed turn angle of  $M$  is about  $117^\circ$  now. We need to assign 0 to other points in this neighborhood, such as point  $N$  and  $P$ , since their contribution is added to  $M$ . According to our experiment,  $T=10$  is a good choice for most of the case.

In our method, the main computation load is to compute the scale measures for all the extreme points in all the directions. In the worst case, the time complexity is  $O(Nn^2)$ , where  $N$  is the number of the height functions and  $n$  is the number of vertices on the curve. When they have been computed, given a scale threshold  $\lambda$ , the visual curvature for all the points can be computed in the complexity of  $O(n)$ .

From the definition of visual curvature, we can see that the arc length parameterization is not needed, through it makes our implementation easier. What we need is just the order of the contour points, whether there are gaps or not makes no difference. This makes our method can deal with very complicated images.

In all our experiments,  $N=128$  and  $\Delta S=1$ .

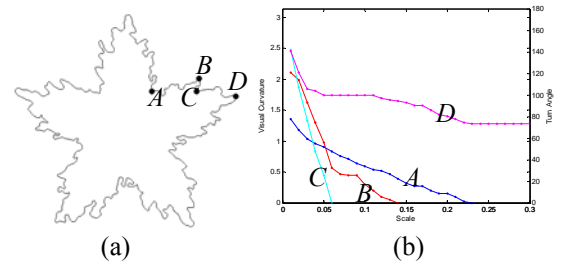


Figure 10. Visual curvatures in different scales

Fig. 10(b) shows the visual curvatures of the four points  $A, B, C, D$  in the Fig. 10(a) calculated in different scales. Obviously, the turn angle of these four points on a pentagram without noise should be  $72^\circ, 0^\circ, 0^\circ$  and  $144^\circ$ , respectively. Because of noise,  $B$  and  $C$  have large turn angles in small scales. For example, when  $\lambda=0.01$ , the turn angles of these points are  $77^\circ, 121^\circ, 142^\circ, 140^\circ$ , respectively. As scale increases, visual curvature decreases. Since  $\lambda(C) < \lambda(B) < \lambda(A) < \lambda(D)$ , the visual curvature of  $C$  vanishes first, then  $B$  and  $A$ , the visual curvature of  $D$  never vanishes since it's a point on the convex hull of the

pentagram. As the value of  $\lambda$  increases, the obtained curvature estimation is not accurate. However, increasing  $\lambda$  is very useful for dominant point detection, e.g., as can be seen in Fig. 10(b). The most dominant point is  $D$  and then  $A$ .

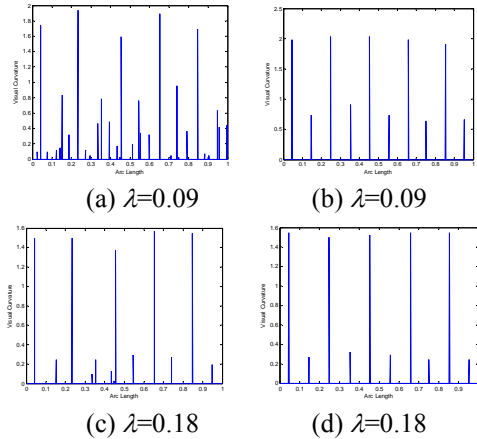


Figure 11. Visual curvature for the two pentagrams in Fig. 2

Fig. 11 demonstrates the visual curvature as arc length functions for two pentagrams in Fig. 2 in two scales. Fig. 11 (a) and Fig.11 (c) is the function of Fig. 2(a); Fig. 11 (b) and Fig.11 (d) is the function of Fig. 2(b).  $A$  is the start point and we follow the contour clockwise. Obviously, there are ten peaks in all graphs; the noise in Fig. 2(a) is suppressed, especially when the scale is large, see Fig. 11(a) and Fig. 11(c).

Fig. 12 demonstrates the multi-scale approximation of Fig. 4(a). As  $\lambda$  increases, the visual curvature of more points vanishes and  $C_\lambda$  becomes simpler until it converges to the boundary curve of its convex hull.

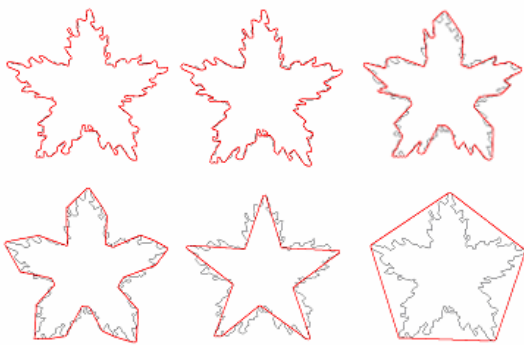


Figure 12. Multi-scale approximation of Fig. 4(a)

## 7. Applications

In this section, we will demonstrate some applications of the multi-scale visual curvature.

### 7.1. Curve Evolution

As  $\lambda$  increases, the  $\lambda$ -scale approximation series  $\{C_\lambda\}$  can be considered as an evolution procedure. Since we just delete the vertices where the visual curvature vanishes, it leads to simplification of shape complexity with no blurring effects and no dislocation of relevant features. Finally, when all the concave segments disappear, the contour converges to the boundary of its convex hull.

Fig. 13 shows the evolution procedure of a horse by gradually deleting the points where visual curvature vanishes. When  $\lambda$  is sufficiently large, the horse is evolved to the boundary curve of its convex hull.

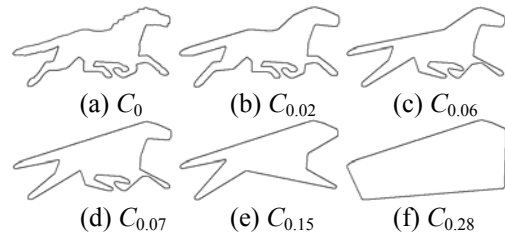


Figure 13. The evolution procedure of a horse

### 7.2. Corner Detection

The multi-scale visual curvature can estimate the curvatures at a continuum of scales. At the same time, it does not modify the original curve. So it can be utilized to detect the corners precisely and robustly.

In our method, a contour point is described both by its visual curvatures and corresponding scales. In a certain scale, we consider the points which digital visual curvature is above a threshold  $DK_0$  as corner points.

Fig. 14 demonstrates the corners of a butterfly detected in different scales. In this experiment, curvature threshold  $DK_0=17\pi/64(48^\circ)$ .

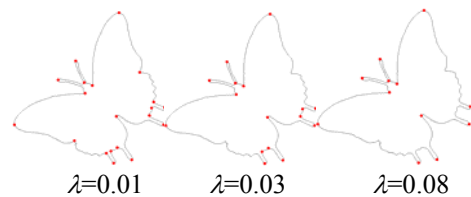


Figure 14. Corners of a butterfly in different scales

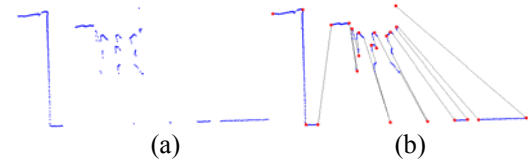


Figure 15. The corners of the raster scanned points

Fig. 15(a) is a raster scanned point set with known order; however, there are many gaps. In Fig. 15(b), we connect these points by line segments and demonstrate the detected corner points at scale 0.01. In this experiment,

$DK_0=33\pi/128(46^\circ)$ .

Figure 16 demonstrates the results of corner detection on 20 kinds of objects, each kind has two images, one is the original image and one is with significant noise.

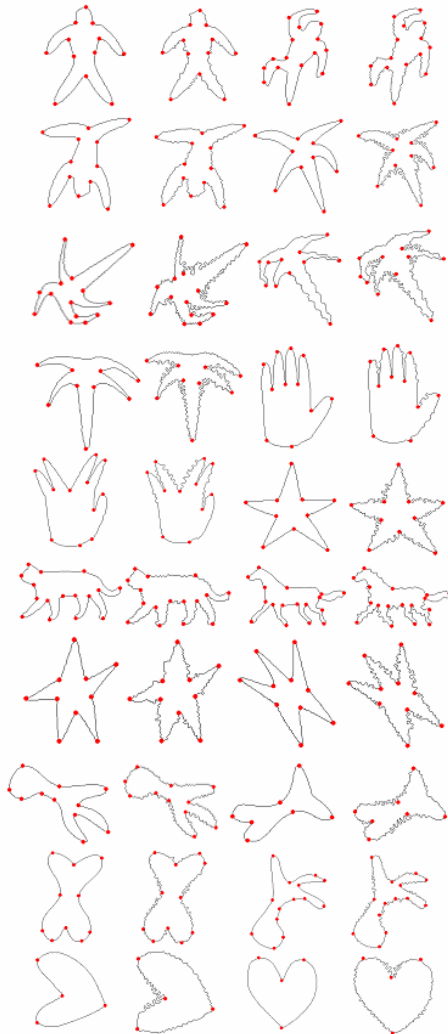


Figure 16. Corner detection of twenty kinds of objects

## 8. Conclusion

This paper proposes a new curvature definition which can be considered to be a geometric explanation of standard curvature. Based on this definition, a natural multi-scale curvature is introduced. Because the scale measure can be defined in different ways, in fact we obtain a series of multi-scale visual curvature.

The properties of the multi-scale visual curvature are investigated and their practical significances are analyzed. Based on these properties, we discussed two kinds of applications of multi-scale visual curvature, corner detection and curve evolution. The experiments show that the multi-scale visual curvature is very robust and intuitive,

and thus is very suitable to visual processing.

## Acknowledgement

This work was supported by the Cultivating Fond for Momentous Scientific Innovation Project of Higher Education in China (Grant no. 705038) and in part by the NSF Grant IIS-0534929 and by DOE Grant DE-FG52-06NA27508.

## References

- [1] M. Worring and A.W.M. Smeulders, Digital Curvature Estimation, CVGIP: Image Understanding, vol. 58, pp. 366-382, 1993
- [2] D. Coeurjolly, M. Serge, and T. Laure. Discrete Curvature based on Osculating Circles Estimation. Lecture Notes in Computer Science, vol. 2059, pp. 303-312, 2001
- [3] Thomas Lewiner, Arc-length Based Curvature Estimator, SIBGRAP'04, pp.250-257, October 2004
- [4] D. G. Lowe, Organization of smooth image curves at multiple scales, in Proc., IEEE ICCV, Tarpon Springs, FL, pp. 558-567, 1988
- [5] A. L. Yuille, Zero crossings on lines of curvature, Comput. Vision Graphics Image Process, vol. 45, pp. 68-87, 1989
- [6] T. Lewiner, J. Gomes Jr., H. Lopes, and M. Craizer. Curvature estimation: Theory and practice. Pr´epublicacoes do Departamento de Matem´atica da PUC-Rio, 2004
- [7] Mokhtarian, F., Mackworth, A.K.: A theory of multi-scale, curvature-based shape representation for planar curves. IEEE Trans. on PAMI, vol. 14, pp. 789-805, 1992
- [8] Yu-Ping Wang, S. L. Lee, and Kazuo Toraichi, Multiscale Curvature-Based Shape Representation Using B-Spline Wavelets. IEEE Transactions on Image Processing, vol. 8, no. 11, 1999
- [9] L. J. Latecki and A. Rosenfeld, Supportedness and Tameness Differentialless Geometry of Plane Curves, Pattern Recognition, vol. 31, no. 5, pp. 607-622, 1998
- [10] Rosenfeld, A. and Johnston, E. Angle Detection on Digital Curves. IEEE Trans. Computers C-22, pp. 875-878, 1973
- [11] N. Katzir, M. Lindenbaum, and M. Porat, "Curve segmentation under partial occlusion," IEEE Trans. PAMI, vol. 16, pp. 513-519, May 1994
- [12] N. Ansari and E. J. Delp, "On detecting dominant points," Pattern Recognition, vol. 24, no. 5, pp. 441-451, 1991.
- [13] Pinheiro, A.M.G.; Izquierdo, E.; Ghanhari, M. Shape matching using a curvature based polygonal approximation in scale-space. International Conference on Image Processing, vol. 2, pp. 538-541, 2000
- [14] A. Bengtsson and J.-O. Eklundh, Shape Representation by Multiscale Contour Approximation, IEEE Trans. PAMI, vol. 13, no.1, 1991
- [15] Gregory Dudekm and John K. Tsotsos, Shape Representation and Recognition from Multi-scale Curvature, CVIU, vol. 68, pp. 170-189, 1997